Gold(I)-Catalyzed Claisen Rearrangement of Allenyl Vinyl Ethers: Missing Transition States Revealed through Evolution of Aromaticity, Au(I) as an Oxophilic Lewis Acid, and Lower Energy Barriers from a High Energy Complex

Dinesh V. Vidhani,*,[†] John W. Cran,[†] Marie E. Krafft,[†] Mariappan Manoharan,[‡] and Igor V. Alabugin*,[†]

[†]Department of Chemistry and Biochemistry, Florida State University, Tallahassee, Florida 32306, United States
[‡]School of Science, Engineering and Mathematics, Bethune-Cookman University, Daytona Beach, Florida 32114, United States

Ⓢ *Supporting Information*

ABSTRACT: Curtin−Hammett analysis of four alternative mechanisms of the gold(I)-catalyzed [3,3] sigmatropic rearrangement of allenyl vinyl ethers by density functional theory calculations reveals that the lowest energy pathway (cation-accelerated oxonia Claisen rearrangement) originates from the second most stable of the four Au(I)-substrate complexes in which gold(I) coordinates to the lone pair of oxygen. This pathway proceeds via a dissociative transition state where the C−O bond cleavage precedes C1−C6 bond formation. The alternative Au(I) coordination at the vinyl π-system produces a more stable but less reactive complex. The two least stable modes of coordination at the allenyl π-system display reactivity that is intermediate between that of the Au(I)−oxygen and the Au(I)−vinyl ether complexes. The unusual electronic features of the four potential energy surfaces (PESs) associated with the four possible mechanisms were probed with intrinsic reaction coordinate calculations in conjunction with nucleus independent chemical shift (NICS(0)) evaluation of aromaticity of the transient structures. The development of aromatic character along the "6-endo" reaction path is modulated via Au-complexation to the extent where both the cyclic intermediate and the associated fragmentation transition state do not correspond to stationary points at the reaction potential energy surface. This analysis explains why the calculated PES for cyclization promoted by coordination of gold(I) to allenyl moiety lacks a discernible intermediate despite proceeding via a highly asynchronous transition state with characteristics of a stepwise "cyclization-mediated" process. Although reaction barriers can be strongly modified by aryl substituents of varying electronic demand, direct comparison of experimental and computational substituent effects is complicated by formation of Au-complexes with the Lewis-basic sites of the substrates.
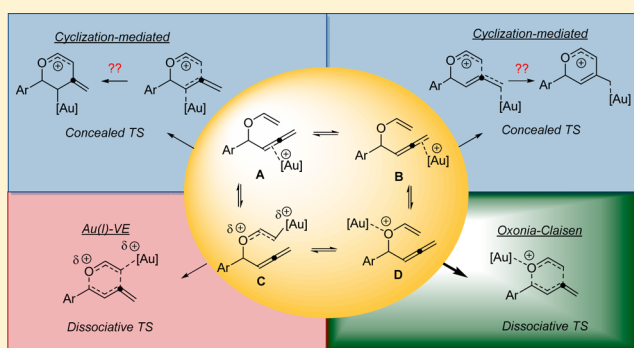
■ INTRODUCTION

The synthetic utility of gold catalysis has grown enormously over the past decade.[1] Gold-catalyzed sigmatropic rearrangements, particularly Cope and Claisen rearrangements, have attracted considerable interest over the past few years.[2] However, not all mechanistic details of these processes are fully understood. For example, Toste and co-workers observed the formation of [1,3] byproducts in the Au-catalyzed propargyl Claisen rearrangement,[3] whereas our group found [1,3] side products in the analogous allenyl-vinyl ether rearrangement.[4] While studying the Au-catalyzed [3,3] rearrangement of pentadienyl vinyl ether compounds, we isolated a significant amount of byproducts formally derived from [1,3] and [3,5] rearrangements (Scheme 1).[5] Formation of the [1,3] and [3,5] products suggests the intermediacy of a dissociative transition state (TS), which is not consistent with the classical model of the Au-catalyzed [3,3]-rearrangement promoted by coordination of gold(I) at the soft π-systems.

A possible explanation is provided by the ionization of C−O bonds well-documented for the other transition metal-catalyzed Claisen type-rearrangements.[6] For example, Hg(II)[7] and Pd(II)[8] complexes were suggested to activate the vinyl ether via oxymercuration/oxypalladation of the alkene followed by cleavage of the C−O bond (Scheme 2). The resulting metal enolate could then react to give the [1,3] product. The Rovis group was able to obtain high yields of [1,3] product in preference to the [3,3]-rearrangement by using oxophilic transition metals such as Cu^{2+} and Ti^{4+}.[9] The activation of the vinyl ether is not limited to transition metals. In a similar study of the Al^{3+} catalyzed [3,3] rearrangement of pentadienyl vinyl ether compounds, Yamamoto observed the formation of

Scheme 1. Examples of [1,3] Products in Au-Catalyzed Rearrangements of Vinyl Ethers

Product Ratios(*Thermal*): 1 : 0 : 0
(*Catalyzed*): 2 : 2 : 1
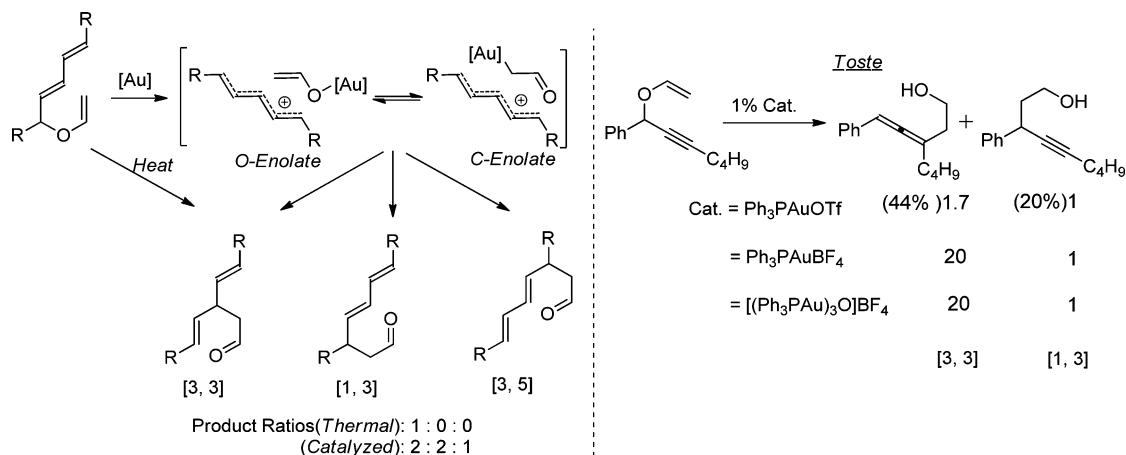
Scheme 2. Two Ways to Involve Vinyl Ether Activation for the Formation of [1,3] Products in Claisen Rearrangements
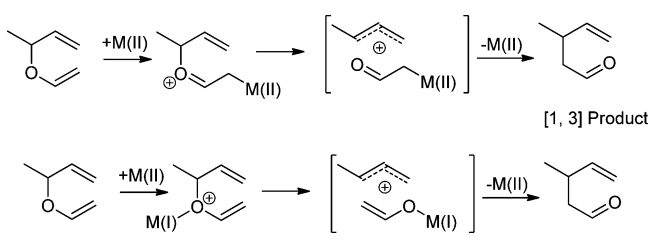
[1,3] and [3,5] byproducts originating from cleavage of the carbinol C−O bond (Scheme 2).[10]

The combination of our own experimental data described above with the literature data suggested that Au(I)-coordination at the vinyl ether (either at the β-carbon or at the oxygen) should be involved at some stage of the gold(I)-catalyzed rearrangement of allenyl and propargyl vinyl ethers in order to explain the observed side products. This hypothesis gains further support in the Au-catalyzed transfer vinylation of alcohols developed by the Tokunaga group, which is suggested to proceed via the activation of the vinyl ether by Au(I),[11] analogously to the earlier reported Pd(OAc)$_2$ or Hg(OAc)$_2$ catalyzed transfer vinylation.[12] Moreover, Roithova et al. has shown that gold(I) would preferentially coordinate to the vinyl ether even in the presence of alkynes and alcohols.[13] To understand the role of Au(I)−vinyl ether complexes in Au catalyzed [3,3] rearrangements, we decided to carry out a computational comparison of the four mechanistic pathways for

the rearrangements based on the four possible coordinating sites of gold(I) to allenyl-vinyl ethers (Figure 1).

The pioneering work of H. Zimmerman and M. Dewar established the important role of transition state aromaticity in thermally allowed pericyclic reactions.[14,15] Indeed, the [3.3]-sigmatropic rearrangement of allyl vinyl ethers[16] involves a well-defined concerted aromatic transition state (TS). However, in [3,3] rearrangements of allenyl vinyl ethers, because of allenic strain and substituents on the carbinol carbon, a larger degree of asynchronicity with a potential transition to a stepwise mechanism is to be expected. In this work, we use two variable parameters, viz., aromaticity and the substituent effects as the probes for the spectrum of possibilities between the two mechanisms. A stepwise mechanism would involve a 1,4-diyl type charged intermediate, which would be less sensitive to the substituents on the carbinol carbon because the C−O bond is not broken in the rate determining step. The transition state for the stepwise mechanism is not expected to display cyclic delocalization associated with aromaticity. On the contrary, the transition state in a concerted pathway would be sensitive to the substituents on the carbinol carbon and also show significant aromatic character.[17]

■ COMPUTATIONAL DETAILS

Because our experimental study showed that the trialkylphosphines served as effective ligands in gold(I)-catalyzed rearrangement, we chose PMe$_3$ ligand for the Au complex throughout our computational study. All stationary point geometries in the uncatalyzed and gold(I)-catalyzed Claisen rearrangements were optimized using the B3LYP functional[18] with LANL2DZ basis set,[19] as implemented in the Gaussian03 package.[20] The same method was successfully used by the
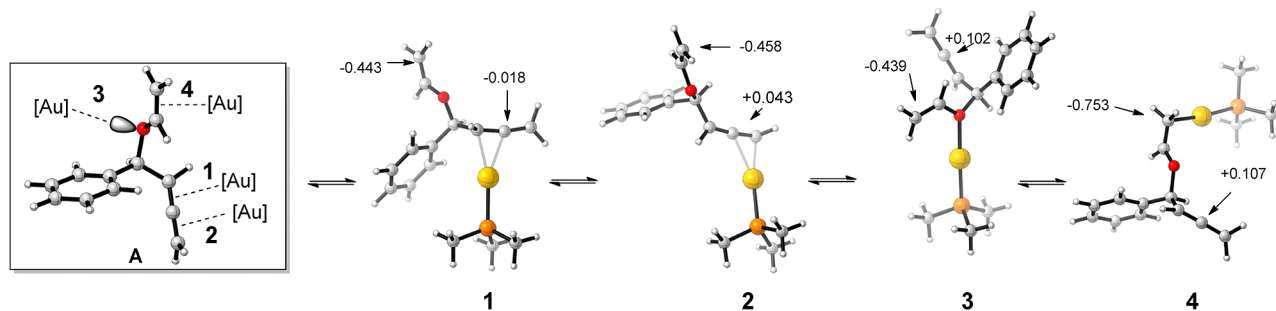

Figure 1. Four coordinating sites of gold(I) in the allenyl vinyl ether system. Natural charges calculated at the B3LYP/LANL2DZ level on the terminal carbon of the vinyl ether and the internal carbon of the allene moiety.

Toste group to calculate the energy parameters for the gold(I)-catalyzed [3,3] rearrangement of propargyl esters and propargyl vinyl ethers.[21] Both activation and reaction energies for the uncatalyzed reactions at this level are in good agreement with B3LYP/6-31G(d,p) values. The choice of B3LYP/LANL2DZ for our systems is supported by a variety of computational studies on the gold(I)-catalyzed rearrangements[22] including the gold(I)-catalyzed Claisen rearrangement of alkynes.[21] The effect of solvent (dichloromethane/CH₂Cl₂) on the reaction barriers was evaluated using single point calculations with the PCM model at the SCRF-B3LYP/LANL2DZ level on the gas-phase geometries. Frequency calculations confirmed that equilibrium geometries have all positive frequencies, whereas transition state (TS) geometries had only one imaginary frequency (see the Supporting Information (SI)). To test for the concerted nature of these reactions, the aromaticity of the selected TSs was examined using nucleus independent chemical shift (NICS(0))[23] and harmonic oscillator model of aromaticity (HOMA) methods. The NICS(0) method introduced by Schleyer is one of the most commonly used, convenient and informative ways to study the aromaticity. It had been successfully applied to a variety of unusual structures, reactive intermediates and transition states and lent itself as a tool for better understanding of the allenic Claisen rearrangements.[23] The NICS(0) were calculated for TSs containing a Au(I)-catalyst at the B3LYP/LANL2DZ level by the NMR-GIAO procedure, whereas the B3LYP/6-311+G(d,p) level was used to compute NICS(0) for noncatalyzed TSs.[24] The HOMA, which is the geometry-based criteria of aromaticity, was calculated using the transition state geometry of the standard Claisen rearrangement of the allyl vinyl ether as a reference point (see SI for the detailed calculations). Intrinsic reaction coordinate (IRC) calculations were used to search for intermediates and additional transition states.

■ RESULTS AND DISCUSSION

1. Uncatalyzed [3,3]-Rearrangements: Twist Boat Vs Twist Chair TS. Before analyzing the gold(I)-catalyzed Claisen rearrangements of aryl-substituted allenyl vinyl ethers, we examined the uncatalyzed version of this process at the B3LYP level with 6-31G(d,p) and LANL2DZ basis sets (eq 1).

$$(1)$$
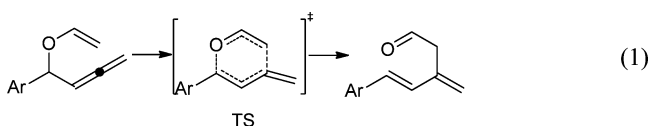
Computations found two possible transition state geometries: the twist-chair (TS$_{Chair-H}$) and the twist-boat (TS$_{Boat-H}$) (Figure 2) in agreement with the earlier findings for the prototypical reactions of this type.[25] Not only are the transition
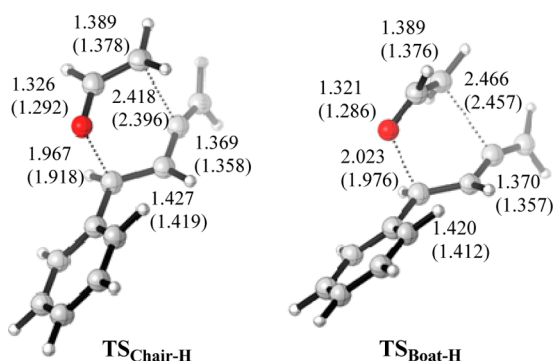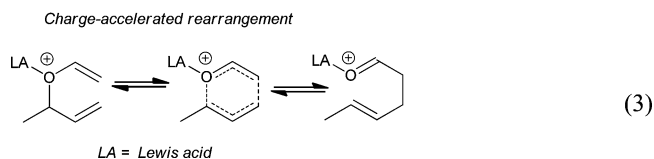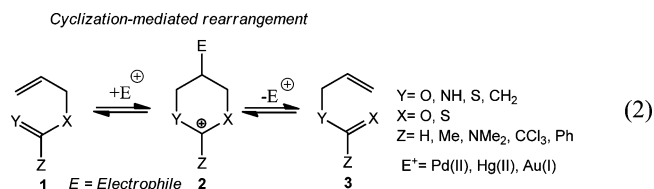

Figure 2. Computed transition state structures (B3LYP/LANL2DZ) for the uncatalyzed Claisen rearrangement of the phenyl-substituted allenyl vinyl ether **5** with selected bond distances (B3LYP/6-31G(d,p) data are in parentheses).

states for the parent Claisen rearrangement asynchronous because of the presence of the heteroatom, but changing from an alkene to allene increases the degree of asynchronicity even further. The bond parameters in the [3,3] rearrangement of allenyl derivatives suggest a more "reactant-like" geometry for the twist-chair conformation compared to the twist-boat TS (Figure 2). Thus, the twist-chair TS correspond to a lower activation barrier (Table 1) relative to twist-boat TS. Furthermore, these calculations support the use of the LANL2DZ basis set for the gold-catalyzed reactions (vide infra) since the activation energies (Table 1) and the TS structures (Figure 2) at the B3LYP/LANL2DZ and B3LYP/6-31G(d,p) levels follow analogous trends.

Although the NICS(0) at the geometric center of the six-membered transition state for the uncatalyzed thermal allenyl vinyl ether rearrangement are slightly less negative than the respective values for the parent Claisen rearrangement (−23 ppm (boat)/−25 ppm (chair), it clear that both the twist-chair and twist-boat TSs for the allenyl system are still aromatic. The less negative NICS(0) value for the twist-chair TS (see NICS(0) in Table 1) suggests a lower degree of aromaticity and, consequently the higher degree of asynchronicity in the twist-boat TS.[26] The allenic strain distorts the TS geometry resulting in smaller NICS(0) than in a typical Claisen rearrangement.[27] The HOMA values were found close to 1.0 relative to TS(Chair) of the allyl vinyl ether, providing structural evidence for the TS aromaticity (see SI for additional details).

2. Gold(I)-Catalyzed Claisen Rearrangements. For the Au(I)PMe₃-catalyzed Claisen rearrangements of aryl-substituted allenyl vinyl ethers, we considered the four mechanisms differentiated by the modes of gold binding (see Figure 1). The first option is the "cyclization-mediated mechanism". This mechanism was first introduced by Henry et al. for the Pd (II)-catalyzed allylic ester rearrangement[28] (eq 2) and subsequently

Cyclization-mediated rearrangement

Y= O, NH, S, CH₂
X= O, S
Z= H, Me, NMe₂, CCl₃, Ph
E⁺= Pd(II), Hg(II), Au(I)

$$(2)$$

1 E = Electrophile **2** **3**

Charge-accelerated rearrangement

$$(3)$$

LA = Lewis acid

expanded by Overman to the Hg(II)- and Pd(II)-catalyzed [3,3] sigmatropic rearrangements.[29] The key feature of this mechanism is the rate-determining intramolecular nucleophilic attack at an electron deficient π-system coordinated to a soft Lewis acid.

In the case of allenes, the cyclization-mediated mechanism can proceed as either a 6-endo or 6-exodig[30] nucleophilic attack of the electron-rich vinyl ether moiety at the allene—Au⁺ complex, depending on whether gold coordinates at the internal or external allene π-bond, respectively (Scheme 3). This attack results in transient formation of a cyclic six-membered intermediate, which may or may not correspond to an energy minimum. The subsequent elimination of the metal

Table 1. Computed Activation and Reaction Energies for the Uncatalyzed Claisen Rearrangement of Various Aryl-Substituted Vinyloxy-buta-1,2-dienes at the B3LYP/LANL2DZ and B3LYP/6-31G(d,p) Levels

		TS	E_a, kcal/mol[a]	NICS(0),[b] ppm	rHOMA
5	Ar = Ph	TS1$_{Chair-H}$[c]	19.9 (21.5)	-17.4	0.99
		TS2$_{Boat-H}$[d]	22.0 (23.1)	-14.5	0.99
6	Ar = p-NH$_2$Ph	TS3$_{Chair-NH2}$[c]	19.8 (20.6)	-16.0	0.97
		TS4$_{Boat-NH2}$[d]	20.9 (23.4)	-13.8	0.96
7	Ar = p-NO$_2$Ph	TS5$_{Chair-NO2}$[c]	19.5 (21.8)	-17.4	0.98
		TS6$_{Boat-NO2}$[d]	21.7 (25.2)	-15.2	0.98

[a]B3LYP/6-31G(d,p) data are given in parentheses. [b]At the GIAO-B3LYP/6-311+G(d,p)//LANL2DZ level. [c]Twist-chair. [d]Twist-boat (see Figure 2).

**Scheme 3. Four Rearrangement Pathways Considered in This Study**
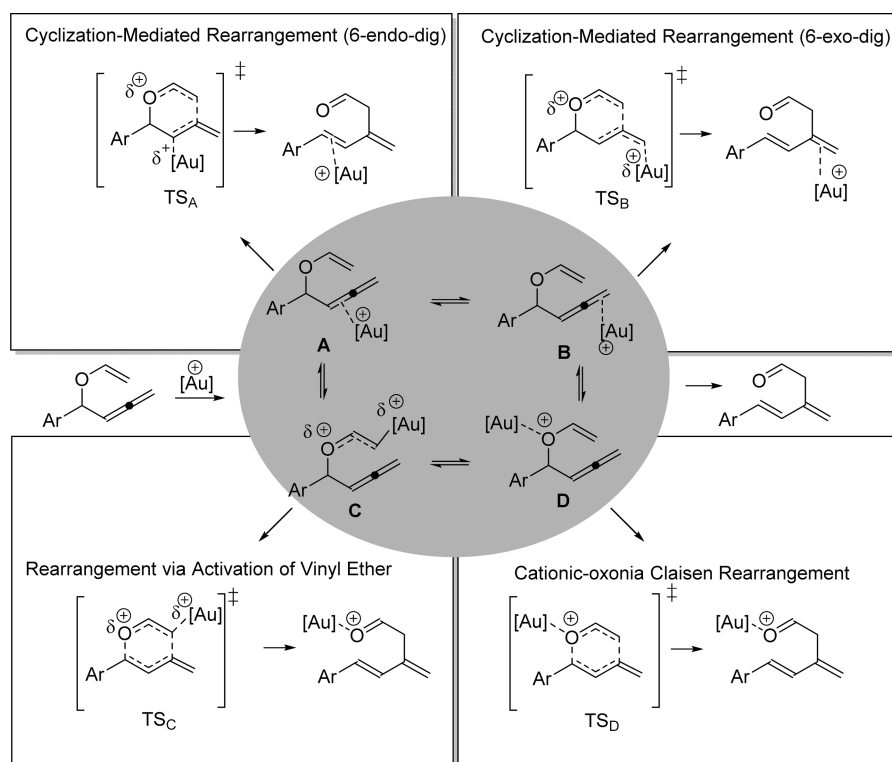
from the cyclic six-membered intermediate via a Grob-type fragmentation gives the product. Formation of a cyclic "intermediate" is less likely if Au$^+$ coordinates at the vinyl ether. Instead, accumulation of partial positive charge on oxygen due to the oxocarbenium character development in the complex leads to polarization and weakening of the central C–O bond (Scheme 3). Another possibility is the cation-accelerated oxonia Claisen rearrangement through the Lewis acid coordination to the heteroatom (eq 3).[31] A highly asynchronous concerted pathway via a "fragmented-TS" initiated by partial C–O bond ionization is expected for such a rearrangement (Scheme 3).

Because the uncatalyzed [3,3] rearrangement of aryl-substituted allenyl vinyl ethers can proceed via either the twist-boat or the twist-chair TS as shown in Figure 2, we considered both conformations for the gold(I)-catalyzed systems as well. Each set of the gold-bound transition states has its own unique features. In particular, the effect of the gold(I)-catalyst on the extent of bond formation and cleavage in the TS is expected to be different. Thus, we will analyze and

compare the key structural aspects and magnetic properties of these TSs to identify the most favorable pathway. We also employed Hammett correlations for systems containing the electronically diverse p-NH$_2$Ph, Ph and p-NO$_2$Ph aryl groups in order to gain deeper insights into the essential features of these mechanisms and into the nature of their transition states.

A. 6-Endodig Cyclization-Mediated Pathway via Au-Bound Allene. In analogy to Overman's "cyclization-mediated" mechanism, the Toste group initially proposed the formation of a six-membered intermediate[5] in the gold(I)-catalyzed propargyl Claisen rearrangement. However, their subsequent computational analysis revealed only a small shoulder in the potential energy profile instead of an energy minimum[21] pointing to an asynchronous but still concerted mechanism for the rearrangement of propargyl substrates. Analogously to these results, we also could not locate the stationary point for the cyclic intermediate corresponding to the 6-endodig closure of the gold-coordinated allenyl ether. Geometry optimizations starting from the cyclic structures led to in silico ring-opening to the respective diene products. IRC computations presented
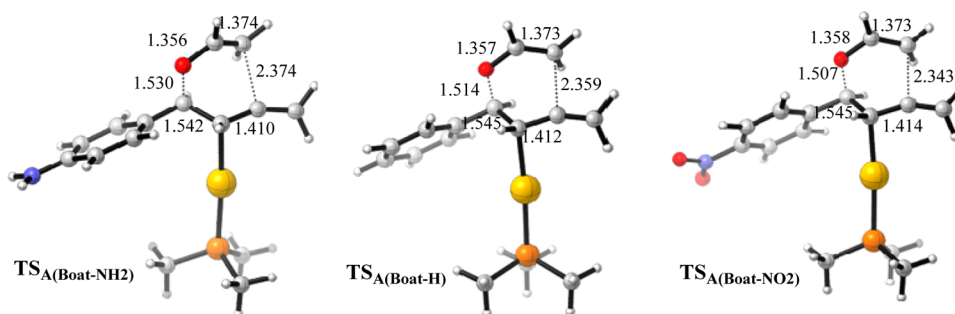
Figure 3. B3LYP/LANL2DZ twist-boat TS geometries for the Au(I)-catalyzed Claisen rearrangements for aryl-substituted vinyloxy-buta-1,2-dienes. The twist-chair geometries are given in the SI.

in Figures 5 and 6 provide a more detailed description of the potential energy surface and still find no intermediate.

Transition State Geometry: Reactant-Like TS. Interestingly, unlike the uncatalyzed reaction, the rearrangement of gold(I)-coordinated allene complex (**1**, Figure 1) prefers the twist-boat (TS$_{A(Boat)}$) to the twist-chair TS (TS$_{A(Chair)}$) (Figure 3). Energies of hyperconjugative interaction in Table 2 illustrate

Table 2. Interaction Energies (kcal/mol) of Lp(O) → π*(C═C) Obtained from Second Order Perturbation Analysis and Natural Atomic Charges (Figure 3)^a

Ar	interaction energy Lp1(O4) → π*(C$_5$═C$_6$)	interaction energy Lp2(O$_4$) → π*(C$_5$═C$_6$)	q(C$_6$)^b	q(C$_2$)^c
PhNH$_2$	6.8	30.7	−0.52	+0.15
	(2.05)	(7.6)	(−0.41)	(+0.12)
Ph	6.7	30.3	−0.52	+0.14
	(2.42)	(7.7)	(−0.41)	(+0.11)
PhNO$_2$	6.6	29.5	−0.51	+0.14
	(2.67)	(7.6)	(−0.40)	(+0.10)

^{a}Values in parentheses correspond to the twist-chair conformation. ^{b}Natural charge on terminal carbon of vinyl ether. ^{c}Natural charge on central carbon of allene.

the stereoelectronic origin of this preference. The lone pair of oxygen overlaps more efficiently with the π-system in the twist-boat TS than in the twist-chair TS. Such delocalization is clearly reflected in the increased negative charges on the terminal carbon of the vinyl ether (C6) in the twist-boat conformation. Concurrently, natural charges indicate that the central allene carbon (C2) is more electrophilic in the twist-boat TSs. The favorable combination of electronic effects accounts for the lower activation energy of the twist-boat path (Table 2).

Importantly, the TS geometries are drastically different between catalyzed and noncatalyzed cyclizations. The Au-catalyzed cyclization displays a very large degree of asynchronicity, resembling very closely the TS expected for a stepwise ("cyclization-induced" in Overman's classification) process. For example, unlike the noncatalyzed version where the C3–O4 distance is increased by 0.48–0.53 Å relative to the reactant, the C3–O4 bond in the Au-catalyzed "6-endo" TS is elongated only by ~0.05 Å.[32,33] Analogously, decrease in the C2–C3 distance associated with the C2═C3 double bond formation is minor for the catalyzed version (B3LYP: 1.54 → 1.53 Å) in comparison with that in the noncatalyzed TS (1.53 → 1.42 Å). On the other hand, the C1–C2 bond length (1.42 Å) is significantly longer for the catalyzed version (compare with 1.37 Å for the noncatalyzed TS). The C1–C6 distances in

the Au-coordinated TS are within the usual range for incipient C···C distances for digonal cyclizations.[34]

Both the lack of structural reorganization between C2 and C3 and between C3 and O4 and the more pronounced C1–C2 elongation suggest a stepwise "cyclization-mediated" pathway, which should involve a six-membered intermediate.[35] Nevertheless, a stationary point corresponding to such an intermediate is absent at the reaction PES, and only a single transition state is involved in this albeit asynchronous but still concerted reaction. The analogously unusual TS features reported by Toste and co-workers for the propargyl Claisen rearrangement[28] suggest that the dichotomy between geometric features of the "cyclization-like TS" and the absence of cyclized intermediate may be common in Au-catalyzed pericyclic reactions.

Computations show that the substituents have little impact on the activation barrier for both twist chair and twist-boat TSs (11.5−11.9 and 8.6−9.1 kcal/mol, respectively, in Table 3; see

Table 3. Activation Energies (kcal/mol) for the Claisen Rearrangement of Allenyl Derivatives in the Gas Phase at the B3LYP/LANL2DZ Level^a

Ar	E_a	$\Delta H^{\ddagger b}$	$\Delta G^{\ddagger b}$	$\Delta E_r^{\ b}$	E_a (solv.)
PhNH$_2$	9.1	8.4	10.9	−37.7	10.6
	(11.9)	(10.8)	(13.6)		(12.6)
Ph	8.9	8.3	11.4	−41.3	10.6
	(11.8)	(10.9)	(14.1)		(12.54)
PhNO$_2$	8.6	8.2	11.9	−36.5	9.5
	(11.5)	(10.7)	(14.1)		(11.6)

^{a}Values in DCM were calculated at the PCM-SCRF-B3LYP/LANL2DZ level using the gas-phase geometries (Figure 3) Values in parentheses correspond to the twist-chair conformation. ^{b}Values correspond to gas phase geometries. ^{c}Values correspond to DCM.
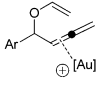
also SI for the M05-2X/LANL2DZ level). For a concerted process, which involves C–O bond breaking, such substituent effects are expected to be more substantial.[36] The low impact of substituents agrees very well with the geometric features of the TSs in indicating that the C–C bond formation proceeds without the C–O bond cleavage, clearly taking the system toward the six-membered intermediate of "cyclization-mediated" processes. However, as we discussed above, despite all the hints that such an intermediate should lie on the rearrangement reaction coordinate, no intermediate is located by the IRC calculations.

Clearly, the absence of a stationary point corresponding to the six-membered intermediate suggesting a concerted pathway and the absence of the substituent effects on the reaction

barrier suggesting a stepwise cyclization-mediated pathway are in a dissonance with each other. This paradoxical situation illustrates the highly unusual features of this reaction that one has to incorporate into one coherent theoretical picture. To gain further insight into these processes, we analyzed electronic and structural features of key structures along the IRC path in conjunction with NICS(0) calculations.

Searching for the Missing Transition State. Subtle structural and electronic effects can expand mechanistic scenarios beyond the textbook "concerted/stepwise" paradigm of pericyclic reactions. For example, bifurcation on a potential energy surface can give rise to a mechanism with two transition states but no discernible intermediate. Such mechanisms correspond to neither a stepwise process nor a concerted process and, instead, are classified within the separate category of "two-step no intermediate" mechanisms. For example, the Caramella group observed that two competing pericyclic pathways shared a common highly asynchronous transition state, the dimerization of methacrolein.[37] Experimental analysis of the 1,2,6-heptatriene → 1,3,6-heptatriene Cope rearrangement, which is topologically similar to the [3,3] rearrangement of allenyl vinyl ethers, showed the properties of both the stepwise as well as the concerted pathway.[38] Later, the Borden group located a single transition state for the process **A → C** via **B** using density functional theory but found evidence for a diradical intermediate **E** with the CASSCF method.[39] The disappearing transition states are not uncommon in complex rearrangements of carbocations.[40]

**Table 4. Computed NICS(0) values at B3LYP/LANL2DZ[a] and B3LYP/6-311+G(d,p) levels[c]**

6-endo-dig Mechanism	Substrate	NICS(0)[a]	NICS(0)[b]
	PhNH$_2$	-8.8 (-11.9)	-9.4 (-13.6)
	Ph	-8.9 (-12.1)	-9.5 (-13.5)
	PhNO$_2$	-8.9 (-12.1)	-9.6 (-13.7)

[a]At the B3LYP/LANL2DZ level (with gold). [b]At the B3LYP/6311+G(d,p)//LANL2DZ level (without gold). [c]Values in parentheses correspond to the twist-chair conformation.

For a stepwise cyclization-mediated pathway, one would anticipate TS aromaticity to be relatively low because of the lack of cyclic electron delocalization. Indeed, the computed NICS(0) for both twist-chair and twist-boat TSs of the 6-endo Au-catalyzed rearrangements suggest that aromaticity is decreased (NICS(0) of −13.5 and −9.5 ppm, respectively, Table 4) relative to the uncatalyzed TSs (Table 1) for all substituents used in this study. We also carried out NICS(0) calculations for the TS geometries without gold and found that, at these geometries, the presence of gold has only a minor effect on TS aromaticity.

Nonetheless, although the NICS(0) suggest that aromaticity is decreased (in a full agreement with the "stepwise" geometric features of this asynchronous TS) relative to the truly concerted noncatalyzed reactions, the aromatic character does not fully disappear despite the aborted delocalization between the C2−C3 bond.[41] In order to investigate the evolution of aromaticity further along the reaction path, we performed NICS(0) calculations for both conformations of the transition state.

In both cases, the NICS(0) value indicated a progressive *increase* in aromaticity *after* the TS state. Moreover, this magnetic evaluation of aromaticity is fully consistent with the observed structural changes leading to more symmetric geometries *beyond* the transition state (Figure 4). However, neither the second TS nor an intermediate were found, and the process remained fully concerted.
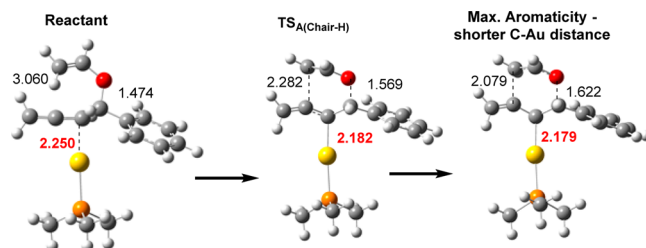

Figure 5. IRC geometries showing the interplay of C1−C6, C3−O4 and C−Au distances at selected PES regions.

IRC calculations also provided the evidence against a "two step/no intermediate" mechanism, which would be expected to give a shallow downhill slope. The nature of electronic and structural reorganization in this part of the PES can be
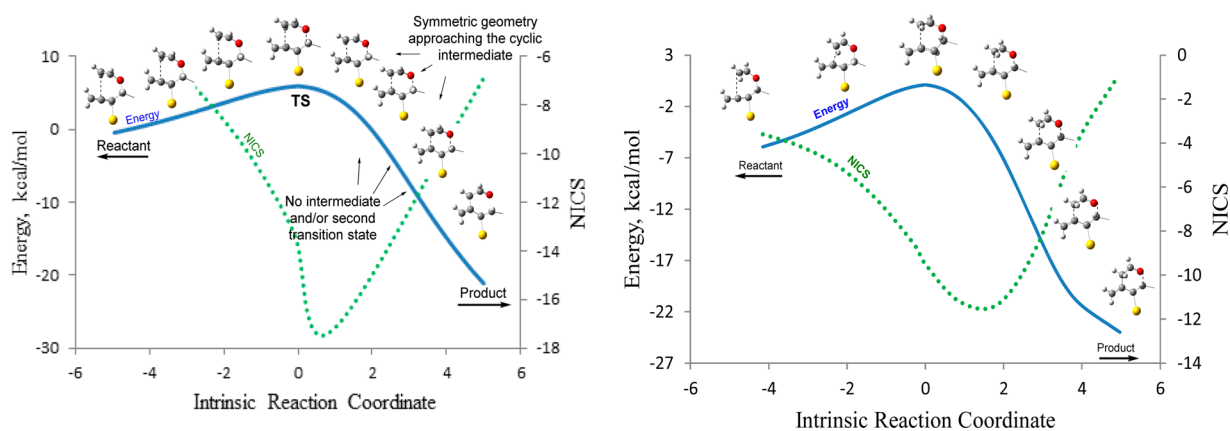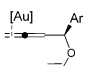

Figure 4. B3LYP/LANL2DZ IRC calculations for the "6-endo" rearrangement of Ph-substituted substrate 5. The solid blue line describes changes in energy. The solid green line corresponds to evolution of aromaticity along the IRC. Top: Twist-Chair TS. Bottom: Twist-Boat TS.
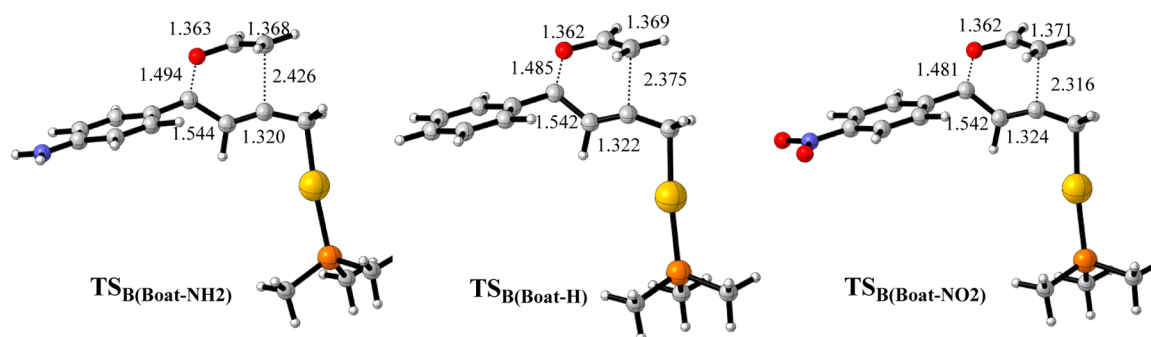
Figure 6. B3LYP/LANL2DZ twist-chair TS geometries for the "6-exodig" Au(I)-catalyzed Claisen-rearrangements of aryl-substituted vinyloxy-buta-1,2-dienes. The twist-chair geometries are given in the SI.

Table 5. Natural Bond Orbital (NBO) Second Order Perturbation n(O) → π*(C=C) Interaction Energies (kcal/mol) and Natural Charges (a.u.) at Selected Atoms in Gold-Catalyzed 6-Exo Transition States[a]

	Interaction Energy Lp1(O)→π*(C=C)	Interaction Energy Lp2(O)→π*(C=C)	$q(C_6)$[b]	$q(C_2)$[c]
R = NH$_2$	6.6	33.5	-0.52	+0.19
	(2.1)	(8.6)	(-0.45)	(+0.16)
R = H	6.5	33.2	-0.52	+0.19
	(2.8)	(8.2)	(-0.41)	(+0.15)
R = NO$_2$	6.4	32.7	-0.52	+0.18
	(3.1)	(7.8)	(-0.41)	(+0.14)

[a]Values in parentheses obtained from twist-chair TSs. [b]Natural charge on terminal carbon of vinyl ether. [c]Natural charge on central carbon of allene.

understood from the changes in the C−Au distance along the IRC path. A stepwise cyclization mediated process with simultaneous barrierless migration of gold(I) to the developing anionic center would result in an apparently concerted but highly asynchronous process. Indeed, the C−Au bond distance in 6-endodig-chair TS reaches the minimum (2.179 Å compared to 2.349 Å in the Au(I)-allene π-complex) after the transition state in the PES region that closely corresponds to the geometry of the putative six-membered intermediate. At this geometry, the anionic character would develop at C2 and get maximum stabilization from interaction with the cationic gold center. This electronic change would lead to selective stabilization of the PES part corresponding to the intermediate and the second TS for the stepwise process.[42] Such stabilization could remove the second activation barrier explaining the anomalous character of the adjacent part of the rearrangement PES and explaining why neither us (for allenes) nor the Toste group (for alkynes)[28] could locate the stationary point for the proposed six-membered intermediate expected for a stepwise cyclization-mediated mechanism. Interestingly, the minimum C−Au distance for the analogous boat TS was found noticeably later (19.7 kcal/mol downhill from the transition state, see the SI section) but the C−Au bond was even shorter (2.16 vs 2.18 Å for chair TS) (Figure 5). The correlation of IRC and NICS(0) mirrored the trend for the 6-endo chair PES with aromaticity fully developing *after* the TS (Figure 4).

B. 6-Exodig Cyclization-Mediated Pathway via Au-Bound Allene. This mechanism is similar to the previous "6-endo" mechanism, but gold(I) migrates to the terminal carbon of the allene; thus, this process can be defined as 6-exo-dig rearrangement (**2**, Figure 1). Potentially, this mechanism could also go through a cyclic intermediate, which subsequently would give the diene product via a Grob-type fragmentation.

However, all attempts to locate a stationary point corresponding to the six-membered intermediate also failed (vide infra).

Transition State Geometries. The twist-boat and the twist-chair 6-exo TSs reveal structural features in the "vinyl ether" moiety (Figure 6) that are similar to those in the 6-endodig pathway. However, changes in the "allene" part are different. For example, changes in the C1−C2 and C2−C3 bond lengths are less pronounced in the 6-exo TSs suggesting the relative inefficiency of cyclic delocalization due to the coordination of gold(I) at the exocyclic carbon. Substituents had a noticeable impact on the transition state geometries. The incipient C1···C6 bond in the TS is shorter in the presence of an electron withdrawing substituent (2.17 Å for nitro vs 2.28 Å for the amino group), indicating that electron acceptors lead to a later TS.

Analogous to the 6-endodig process, the lone pairs on oxygen are delocalized in the π-system of the alkene to a greater extent in the twist-boat conformation (TS$_{B(Boat)}$) than in the

Table 6. Activation Energies (kcal/mol) for the Claisen Rearrangement of Allenyl Derivatives (Ar = *p*-NH$_2$Ph, Ph, and *p*-NO$_2$Ph)[a]

	E_a	$\Delta H^{\ddagger}$	$\Delta G^{\ddagger}$	ΔE_r	E_a(solv.)
R = NH$_2$	6.5	5.6	7.9	-47.6	8.6
	(13.7)	(12.6)	(14.6)		(15.7)
R = H	6.8	6.0	8.6	-41.1	9.7
	(14.4)	(13.4)	(16.1)		(16.4)
R = NO$_2$	7.4	6.7	9.4	-38.7	10.7
	(15.3)	(14.4)	(17.0)		(17.4)

[a]Energies in CH$_2$Cl$_2$ are calculated at the PCM-SCRF-B3LYP/LANL2DZ level on the gas-phase geometries. Values in parentheses obtained from twist-chair TSs.
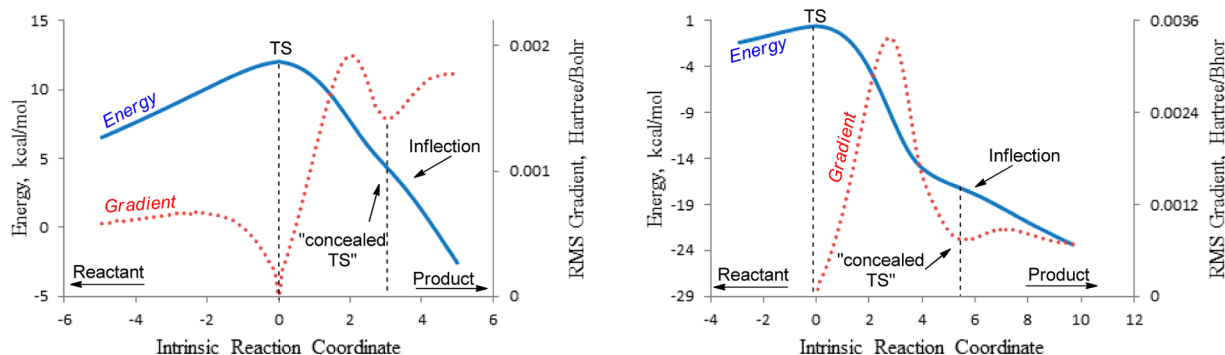
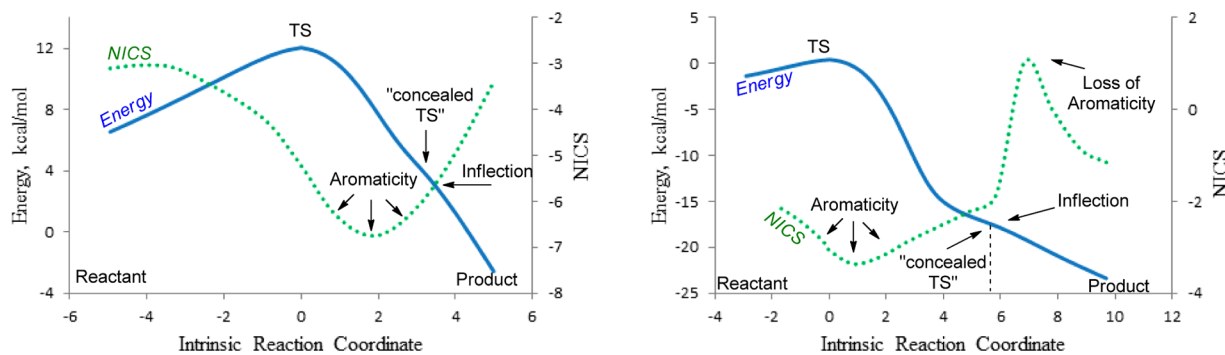**Figure 7.** IRC energies and gradients for the twist-chair (left) and twist-boat (right) 6-exo rearrangements.

Figure 8. IRC calculations performed at the B3LYP/LANL2DZ level for the gold(I)-coordinated Ph-substituted substrate **5**. The solid blue line describes changes in energy. The green dotted line corresponds to evolution of aromaticity along the IRC. Left and right figures correspond to the twist-chair and twist-boat conformations, respectively.

twist-chair ($TS_{B(Chair)}$). The hyperconjugative interaction energy ($n(O) \rightarrow \pi^*(C=C)$) is roughly four times higher in the twist-boat compared to the twist-chair, which can be confirmed by an enhanced NBO negative charge on the terminal carbon of vinyl ether in the twist-boat conformation (Table 5). In addition, the reacting allene carbon is more electrophilic in a twist-boat than in a twist-chair conformation reflected in NBO charges (Table 5). The stereoelectronic features described above explains why the twist-boat conformation is preferred over the twist-chair in the 6-exo path as well (Table 6).

Is 6-Exodig a Concerted Process? Earlier, the IRC and NICS(0) calculations helped to identify the concealed transition state in 6-endodig processes. In this section, we will analyze the nature of transition states for the 6-exo path.

Despite a continuous decrease in the C1−C6 distance along the IRC path on the product side of the TS, neither a six-membered intermediate nor any other energy minima are present (Figure 7). However, in contrast to the 6-endo path, the calculations showed an inflection along the 6-exo IRC path. The RMS gradient showed a minima for this inflection point corresponding to the "invisible" second transition state related to the Grob-type fragmentation. The inflection is more pronounced for the twist-boat path (Figure 7).

As expected from the TS geometries, the computed NICS(0) for both TS conformations for the 6-exo process indicated considerably lower aromaticity (Figure 8).[43] The more distorted twist-boat conformation showed less negative NICS. Analogous to the 6-endodig process, the NICS(0) values suggested a *progressive increase in aromaticity* after the TS state. Interestingly, the 6-exoboat conformation showed a decrease in

aromaticity near the inflection point corresponding to the product-side of the concealed transition state (Figure 8).

The NICS(0) values were insensitive to the nature of the substituents on the carbinol carbon suggesting that the C4−O3 bond does not contribute significantly to cyclic delocalization. This is consistent with the relatively low degree of C4−O3 bond elongation in the TSs. Thus, magnetically, this mechanism shows little aromaticity compared to the uncatalyzed rearrangement. The geometric criteria, the HOMA values, also suggested a lower aromaticity compared to the standard thermal allyl vinyl ether rearrangement (see the SI for additional information). These results put the asynchronous 6-exo mechanism closer to the stepwise pathway.

C. Rearrangement via Activation of the Vinyl Ether. Formation of the [1,3] side product is generally observed in acid catalyzed Claisen rearrangements[10] and the amino-Claisen rearrangement.[44] The same intermediate was also proposed to give a typical [3,3] rearrangement via a charge-induced pathway as shown in eq 3. Since Au(I) is a soft Lewis acid, it is more likely to coordinate with a softer π-base, the vinyl ether or allene, rather than the oxygen, as found by the ESI-mass spectrometry and the computational studies of Schwarz and co-workers.[13] In this section, we explore the possibility of the [3,3] product emanating from the most stable of the four gold(I)-substrate complexes shown in Figure 1.

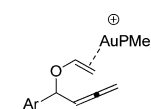*Transition State Geometry: Fragmented Product-Like TS.* Contrary to the uncatalyzed reaction and the previous two mechanisms, the effect of the gold(I)-catalyst on the bond forming and cleaving processes is profound. Notably, the C1···C2 (allene), C3···O4 and C5···C6 (alkene) bonds were cleaved to a much greater extent in TS_C compared to the uncatalyzed TS (Figure 2). A significant increase in the TS
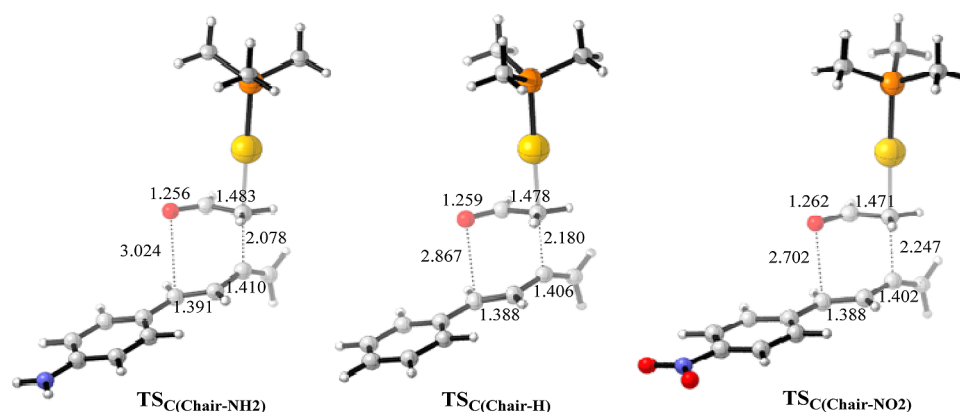
Figure 9. B3LYP/LANL2DZ twist-chair TS geometries for the gold(I)-catalyzed Claisen-rearrangements of aryl-substituted vinyloxy-buta-1,2-dienes in polarization-induced mechanism. The twist-boat geometries are given in the SI.

Table 7. Activation Parameters and Reaction Energies (kcal/mol) for the Gold(I) Catalyzed [3,3]-Rearrangement of Allene Derivatives Calculated at the B3LYP/LANL2DZ level

	$E_a{}^a$	$\Delta H^{\neq a}$	$\Delta G^{\neq a}$	ΔE_r	$E_a(CH_2Cl_2)$	$NICS(0)^b$
R = NH$_2$	22.0 21.6)	21.0 (20.5)	21.5 (21.5)	-28.3	18.9 (17.8)	N.A (-6.1)
R = OMe	24.3 22.8)	22.9 (21.6)	23.6 (23.2)	-29.0	21.1 (20.1)	-4.58 (-6.3)
R=Me	25.8 (24.6)	24.9 (23.8)	23.8 (22.8)	-28.8	22.8 (22.0)	-5.14 (-7.1)
R = H	26.5 (25.4)	25.0 (24.0)	25.1 (24.2)	-29.1	23.2 (22.4)	-5.5 (-7.5)
R = Cl	26.1 (25.0)	24.5 (23.5)	24.6 (23.9)	-30.1	23.5 (22.8)	-5.9 (-7.7)
R = CN	26.5 (25.5)	25.0 (24.1)	26.0 (25.2)	-31.1	23.0 (22.3)	-6.7 (-8.5)
R = NO$_2$	27.0 (26.1)	25.4 (24.6)	25.9 (24.2)	-31.9	24.7 (24.1)	-7.2 (-9.3)

^{a}In the gas phase. ^{b}B3LYP/6-311+G(d,p) level. Values in parentheses correspond to twist-chair conformation.

distances for the three breaking bonds compared to the reactant (C1–C2: 1.33 → 1.40 Å, C3–O4: 1.58 → 2.75–3.02 Å and C5–C6: 1.41 →1.47 Å, respectively) also indicates product-like transition states (Figure 9).

The unusually long carbinol C–O bond is consistent with the observation of [1,3] byproducts in such gold-catalyzed rearrangements. In addition, the substituents on the carbinol carbon had a profound impact on the bond formation and cleavage in **TS$_C$**. In concurrence with the strength of the C3–O4 bond, the asynchronicity decreases for the electron-poor aryl groups (Figure 9). The substituent effects on the rearrangement barrier are relatively large, with the calculated activation barriers being higher than for the earlier discussed mechanisms (Table 7 and see SI for the reaction energy profile).

Concerted vs Stepwise. The structural features of the TSs in this mechanism are very sensitive to the nature of substituents on the carbinol carbon. A shift toward a less asynchronous transition state is observed upon an increase in the electron acceptor properties of the substituents. Since the twist-chair TSs provides a lower energy pathway compared to twist-boat TSs, only the twist-chair was considered for the remaining part of the NICS(0) discussion. Because of considerable C3–O4 cleavage, these TSs are significantly less aromatic than the TSs for the uncatalyzed reaction (Table 1).

Interestingly, a strong correlation was observed between NICS(0) and Hammett Substituent constants (see the SI part), suggesting that aromaticity of these TSs is tunable and that electron withdrawing substituents shift the mechanism toward less-asynchronous transition states in order to avoid development of positive charge on carbinol carbon. The IRC calculations for the gold(I)-coordinated Ph-substituted substrate **5** indicated a concerted process with no sign of any intermediate along the reaction coordinate for both the
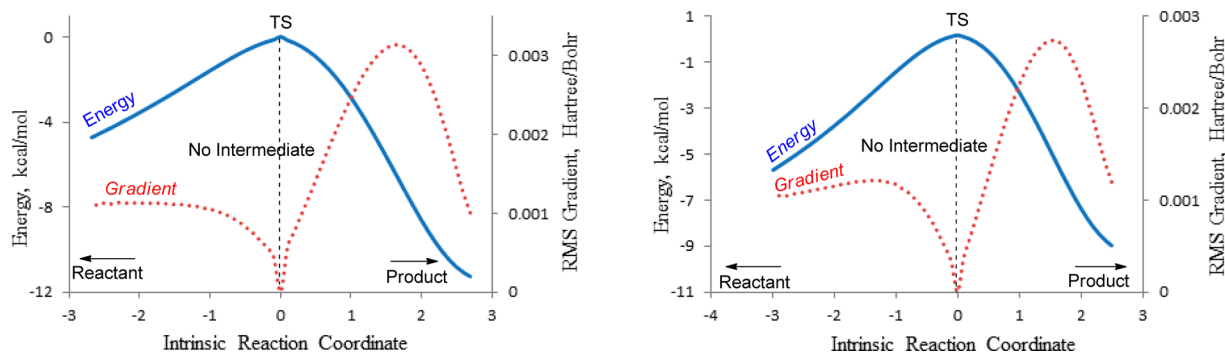
Figure 10. IRC energies and gradients for the Au(I)−VE rearrangement in the Ph-substituted substrate. Left: the twist-chair path. Right: the twist-boat path.
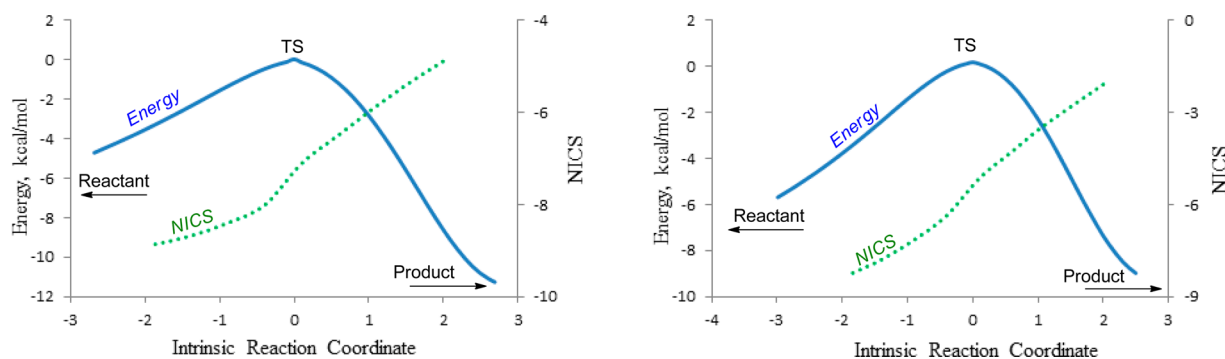
Figure 11. B3LYP/LANL2DZ IRC calculations for the Au(I)−VE rearrangement Ph-substituted substrate **5**. The solid blue line describes changes in energy. The green dotted line corresponds to evolution of aromaticity along the IRC. Left: the twist-chair path. Right: the twist-boat path.
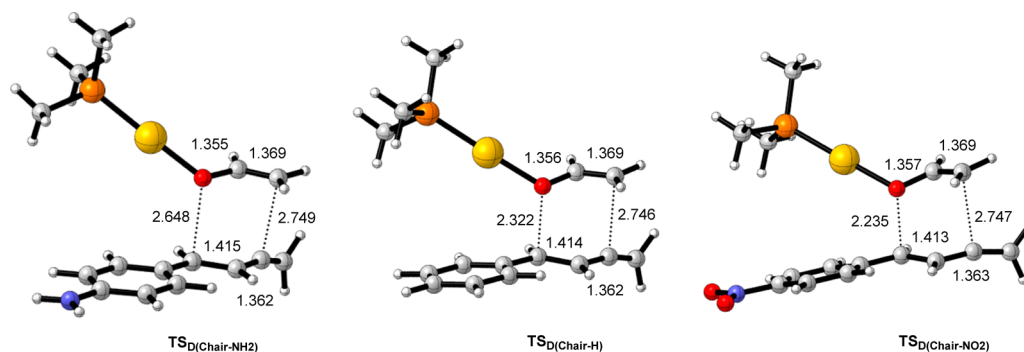
Figure 12. Computed TSs for the gold(I)-catalyzed Claisen-rearrangements for different aryl-substituted vinyloxy-buta-1,2-diene derivatives in polarization-induced mechanism (B3LYP/LANL2DZ).

conformations (Figure 10). The correlation of IRC energies and NICS(0) suggested the rapid loss of aromaticity on the product-side of the transition state (Figure 11).

Overall, the IRC and NICS data suggest that Au(I)−VE complex-mediated rearrangement follows a high energy asynchronous pathway with a "dissociative" TS. The substituents on the carbinol carbon are predicted to show a profound effect on the nature of the transition state and the reaction barriers.

D. Cation-Accelerated Oxonia Claisen Rearrangement. The charge-acceleration due to coordination of the Lewis acid to the heteroatom in the Claisen rearrangement was initially reported by Takai et al.[31] A similar acceleration was observed by the Evans group in an anionic oxy-Cope rearrangement where the negatively charged oxygen dramatically accelerated the reaction compared to the neutral hydroxyl group.[45]

Dissociative-Like Transition State Geometries. Analogous to the rearrangement via activation of the vinyl ether, coordination of gold(I) to the lone pair of oxygen led to significant elongation of the carbinol C3−O4 bond in the reactant compared to the uncomplexed substrate (1.49 → 1.56 Å). The activation of the carbinol C3−O4 bond depends strongly on the substituents (see the SI) (Figure 12).

The electron donating amino group promoted this cleavage and drove the reaction via a highly asynchronous pathway, while the electron withdrawing nitro group disfavored this cleavage by directing the reaction through a more synchronous pathway. The effect of substituents on the other bond-cleaving and bond-forming processes is relatively small, and other structural parameters are relatively close to the concerted-uncatalyzed rearrangement. In this case, a cationic version of the [3,3] rearrangement should be a concerted process proceeding via a dissociative-like[46,47] or a highly asynchronous

Table 8. Activation Energies (kcal/mol) for the Claisen Rearrangement of Allenyl Derivatives in the Gas Phase at the B3LYP/LANL2DZ Level[a]

Ar	E_a	$\Delta H^{\ddagger}$	$\Delta G^{\ddagger}$	ΔE_r	E_a (solv)[b]	NICS(0)[c]	NICS(0)[d]
PhNH₂	2.7	1.6	2.4	−37.4	1.4	−5.5	−8.0
	(1.0)	(0.0)	(1.0)		(0.0)[d]	(−7.6)	(−11.4)
Ph	6.8	5.3	5.8	−39.3	7.1	−9.3	−12.1
	(3.6)	(2.3)	(3.7)		(3.6)	(−10.9)	(−13.7)
PhNO₂	8.8	7.2	7.6	−40.8	9.1	−10.6	−13.4
	(4.6)	(3.7)	(4.2)			(−12.0)	(−14.2)

[a]Values in DCM were calculated at the PCM-SCRF-B3LYP/LANL2DZ level using gas-phase geometries. [b]Values correspond to DCM. [c]Values computed at B3LYP/LANL2DZ level. [d]Values computed at B3LYP/6-311+G(d,p) level. [e]Barrierless reaction in solvent. Values in parentheses correspond to twist-chair conformation.
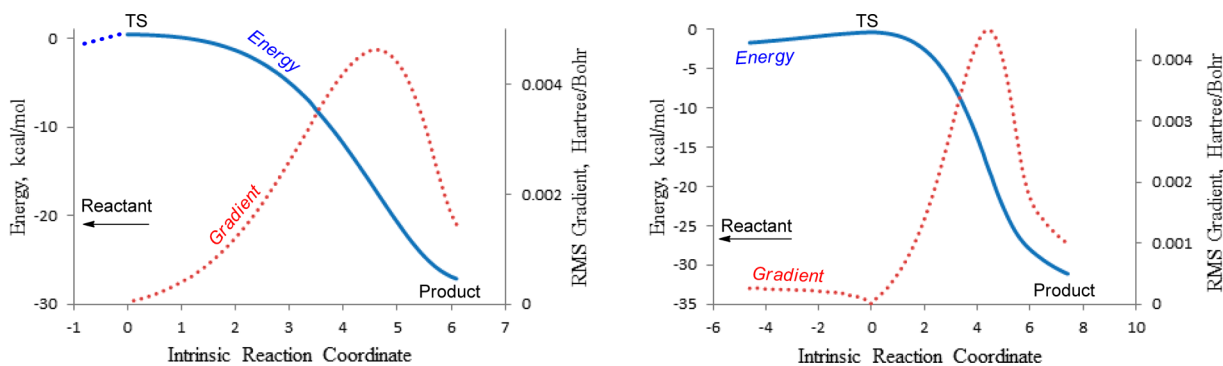
Figure 13. IRC energies and gradients for the Au(I)−VE rearrangement in the gold(I)-coordinated Ph-substituted substrate **5**. The left and the right figures correspond to the twist-chair and the twist-boat conformations respectively.
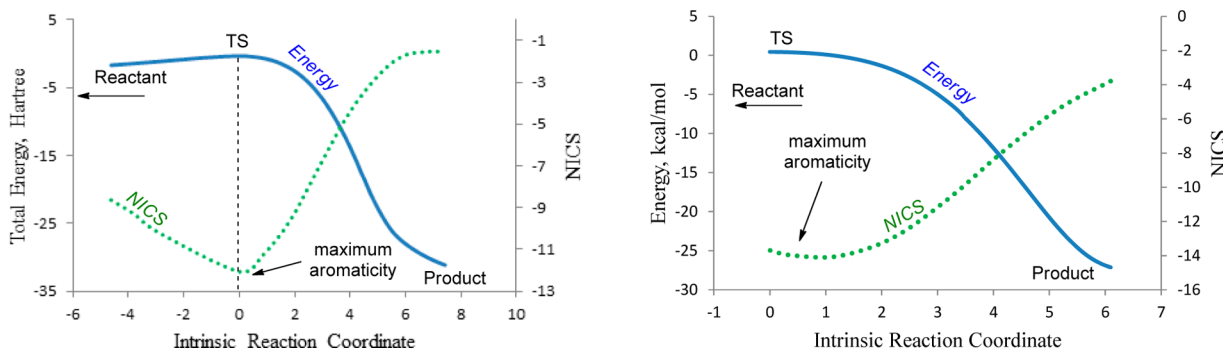
Figure 14. IRC energies for the twist-chair (right) and twist-boat (left) cation-accelerated oxonia Claisen rearrangement shown using a solid blue line. Green dashed lines correspond to evolution of aromaticity along the PES.

transition state. The computed NICS(0) values suggested moderately aromatic transition states (Table 8).

The concerted nature of this process was further confirmed by the IRC calculation that was performed on the B3LYP/LANL2DZ level for the phenyl substituent that showed no sign of an intermediate for both the conformations (Figure 13). The evolution of aromaticity along the PES suggested a symmetric structure near the transition state despite unusually long C3−O4 and C1−C6 bonds (Figure 14).

Thus overall, from activation energies, IRC and NICS(0), the gold(I)-catalyzed oxonia Claisen rearrangement is predicted to follow a low energy asynchronous pathway with a "dissociative" TS. Analogous to the gold(I)−VE mechanism, the substituents on the carbinol carbon are predicted to show a profound effect on the nature of the transition state and the reaction barriers.

E. Comparison of the Four Mechanisms. Using Curtin−Hammett correction, we determined the barrier energies for the four pathways relative to the most stable complex (Figures 15

and 16). Among the four mechanisms discussed above, the gold(I)-coordinated vinyl ether reactant is the most stable, but the lowest energy pathway emanated from the gold(I)-coordination to the oxygen [−35.2 and −32.0] followed by the 6-exodig (twist-boat) [−28.7] > 6-endodig (twist-boat) [−26.1] > 6-endodig (twist-chair) [−23.1] > 6-exodig (twist-chair) [−21.2] ∼ gold(I)−VE-pathway (twist-chair) [−21.1] > gold(I)−VE-pathway (twist-boat) [−20.1] (all energies are in kcal/mol relative to the isolated reactants).

After the Curtin−Hammett correction, oxonia-Claisen and Au(I)−VE mechanisms showed a positive slope suggesting a build-up of cationic character on the carbinol carbon (Figure 16). The 6-exo and 6-endo mechanisms showed an opposite trend with a small bias toward electron acceptors. Interestingly, the lowest energy cation-accelerated oxonia Claisen pathway originates from the higher energy Au(I)−oxygen complex rather than the most stable Au(I)−VE complex. Calculations performed at the M05-2X/LANL2DZ and MP2/LANL2DZ//
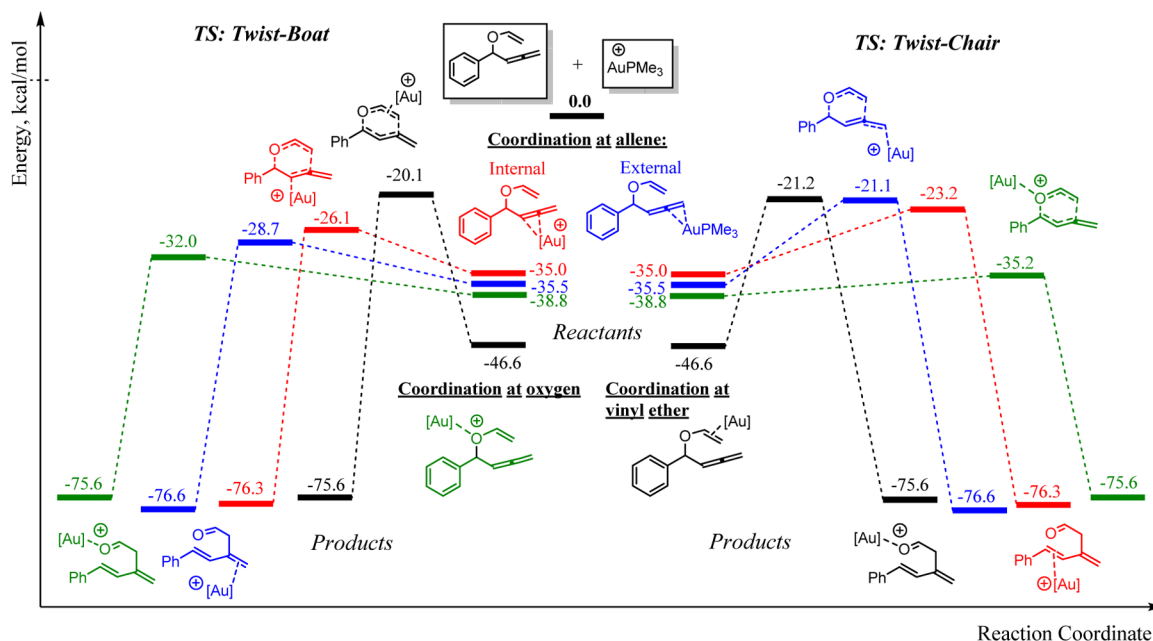
Figure 15. Curtin−Hammett analysis for the relative energies of the four mechanisms for the [3,3]-rearrangement of vinyloxy-but-1,2-diene (see Scheme 1).
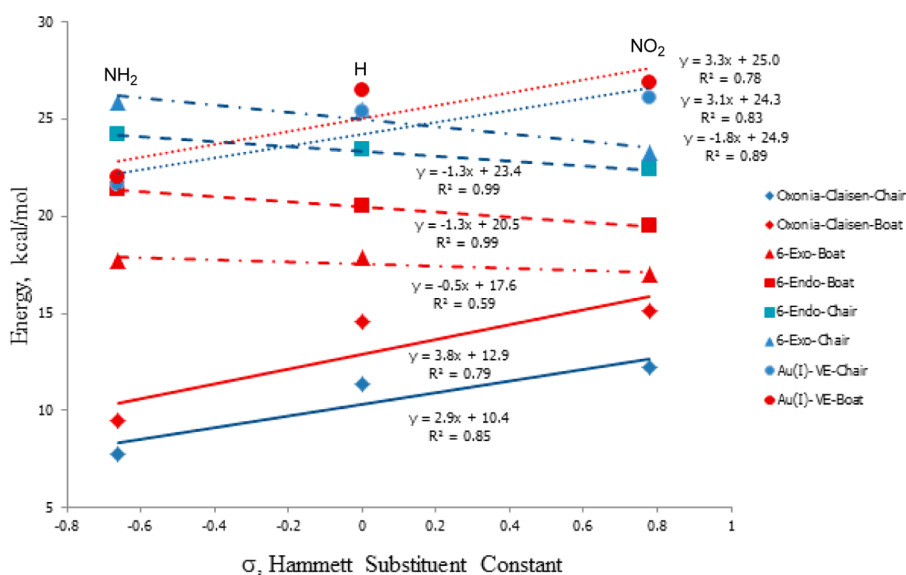

Figure 16. Hammett plot after the Curtin−Hammett corrections. Blue and red colors correspond to the twist-chair and the twist-boat conformations, respectively. Diamonds, oxonia-Claisen; triangles, 6-exo; squares, 6-endo; and circles, Au(I)−VE mechanisms. Energies are given in kcal/mol relative to the energy of the most stable Au-substrate complex.

B3LYP/LANL2DZ levels retained the preference for the oxonia Claisen pathway (see Table S2 in the SI) but suggested that the "6-endo" and "6-exo" pathways remain a viable possibility. The potential energy surfaces for these three mechanisms converge when electron acceptors are attached on the carbinol carbon. Electron acceptors lead to a mechanistic shift toward a less asynchronous path in order to avoid the positive charge development on the carbinol carbon.

3. Correlation of Theoretical and Experimental Studies. Our previous experimental study[4] showed that under thermal conditions, the uncatalyzed allenyl vinyl ether rearrangement took approximately 1.5 h for 60% conversion at 110 °C. This observation is consistent with the relatively high values for the calculated barriers (Table 1). In agreement with

the forbidden nature of [1,3] sigmatropic shifts according to the Woodward−Hoffmann rules, no [1,3] side product was observed under thermal conditions.[48]

In contrast, the Au-catalyzed reactions are complete within minutes at room temperature. The short reaction times under the ambient conditions are consistent with the low barriers calculated for the oxonia pathway. The significant substituent effects predicted for this mechanism were consistent with the slower reactions of substrates with the electron acceptor substituents on the carbinol carbon (Table 9).[4] However, the decelerating effect of the nitrile substituent was surprisingly large. Even more surprising was the experimental observation that the electron-donating substituents on the carbinol carbon

Table 9. Effect of Substituents on the Gold(I)-Catalyzed Allenyl Vinyl Ether Rearrangement[4]
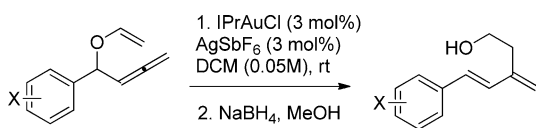
entry	substrate (X)	time	yield[a] (%)
1	H	25 min	86
2	4-OMe	5 h	<40
3	4-Me	12 min	70
4	4-F	30 min	75
5	4-Cl	25 min	80
6[b]	4-CN	25 min	trace

[a]Isolated yield (average of 3 runs). [b]93% in 9 h when refluxed in DCM.

slowed down the rearrangement. These observations led us to explore the role of Au−π and Au−lone pair interactions.

The experimental study of additives on the reaction rate confirmed the importance of the cation−lone pair and the cation−π interaction in Au-catalyzed rearrangements.[49] The alkyl-substitued allenyl vinyl ether **8** was chosen to avoid interactions arising from unproductive sites on the substrate. The reaction was then performed in the presence of additives with varying π-donor strength. Since complete conversion was observed within 30 min for most of the substrates, the reaction was stopped after 10 min, and the product yields were determined by NMR (Table 10).

Table 10. Effect of Additives on Allenyl Vinyl Ether Rearrangement[4]
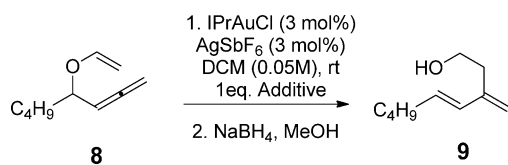
entry	additive	% conv.
1	aniline	
2	benzonitrile	31
3	anisole	71
4	toluene	81
5	benzene	90
6	none	100
7	chlorobenzene	98
8	nitrobenzene	91

As expected, the electron-rich aromatic rings started to compete with the allene for coordination with the Au(I) catalyst. This competition accounts for the unexpected deceleration in the rate of reaction when electron releasing groups are present on the aromatic ring of the substrates. On the other hand, benzonitrile, despite the electron-poor ring, can strongly coordinate with gold(I) via the nitrile lone pair. Indeed, significant reaction inhibition was observed when benzonitrile was used as an additive. This finding accounts for the anomalously low reactivity of the CN-substituted substrate (entry 6, Table 9).

The concerted nature of this rearrangement is also consistent with the unsuccessful attempts to trap the six-membered intermediate with methanol. A similar observation was made by the Toste group and our group in the case of propargyl vinyl ethers. This observation further validates the concerted cation-accelerated oxonia-Claisen pathway as a viable possibility, which is consistent with the experimental results.

Finally, the absence of the [1,3] side products in these reactions is consistent with the asynchronous and highly dissociative but still concerted mechanism. It can also explain why for the more electrophilic AuSbF₆ catalyst, a significant amount (up to 33%) of these byproducts was observed.[4] More electrophilic catalysts are likely to lead to an even more substantial elongation of the carbinol C−O bond and subsequent ionization leading to the [1,3] product.

■ SUMMARY

In summary, computational studies of the Au-catalyzed allenyl vinyl ether rearrangement provided deeper insights into the fundamental factors governing the efficiency of Au(I)-catalyzed reactions. Unexpectedly, the product was found to originate from the higher energy Au(I)−oxygen complex, reacting via a low barrier cation-accelerated oxonia Claisen pathway, instead of the more stable Au(I)−VE complex.

Use of aromaticity as a tracking device allowed us to detect the "missing" transition states for the "cyclization-mediated" 6-endo and 6-exo rearrangement, and identify the key change in the Au-substrate coordination mode, which conceals this TS and the related intermediate in the PES continuum. Not only does this observation reveal the reasons for the apparent dichotomy between the highly asynchronous TS expected to provide a six-membered intermediate and the lack of such intermediate in the concerted path, but it also identifies a conceptually interesting new approach to selective TS stabilization in the Au-catalyzed reaction via the fine-tuning of Au−substrate interactions.

Finally, the accelerating effect of electron donors predicted by the computational study is masked by the unproductive coordination of Au(I) to either the electron rich π-systems or the heteroatomic Lewis bases. Decreased reaction rates in the presence of *external* donor additives provided experimental evidence to this conclusion and illustrated the unproductive role that the stabilization of the starting materials may play in the Au-catalyzed processes.

■ ASSOCIATED CONTENT

Ⓢ Supporting Information

Geometries and energies of all transition states. Reaction energy profiles for all four mechanisms of the [3,3]-rearrangement of vinyloxy-but-1,2-dienes. Curtin−Hammett analysis for the four mechanisms of [3,3]-rearrangement of vinyloxy-but-1,2-diene. Correlation of Hammett substituent constants with activation barriers. Details and results of HOMA calculations. Changes in the C−Au distances along the IRC potential energy surface in 6-endodig mechanism. Additional experimental details. This material is available free of charge via the Internet at http://pubs.acs.org.

■ AUTHOR INFORMATION

Corresponding Author
*E-mail: alabugin@chem.fsu.edu.

Notes
The authors declare no competing financial interest.

■ REFERENCES

(1) (a) Selected reviews: Hashmi, A. S. K. *Chem. Rev.* **2007**, *107*, 3180. (b) Nolan, S. P *Acc. Chem. Res.* **2011**, *44*, 91. (c) Krause, N.; Winter, C. *Chem. Rev.* **2011**, *111*, 1994. (d) Li, Z.; Brouwer, C.; He, C. *Chem. Rev.* **2008**, *108*, 3239. (e) Jiménez-Núñez, E.; Echavarren, A. M. *Chem. Rev.* **2008**, *108*, 3326.

(2) (a) Istrate, F. M.; Gagosz, F. *Beilstein J. Org. Chem.* **2011**, *7*, 878. (b) Sherry, B. D.; Toste, F. D. *J. Am. Chem. Soc.* **2004**, *126*, 15978. (c) Shi, Z.; He, C. *J. Am. Chem. Soc.* **2004**, *126*, 5964. (d) Shi, Z.; He, C. *J. Am. Chem. Soc.* **2004**, *126*, 13596. (e) Shi, Z.; He, C. *J. Org. Chem.* **2004**, *69*, 3669. (f) Reich, N. W.; Yang, C.-G.; Shi, Z.; He, C. *Synlett* **2006**, 1278. (g) Suhre, M. H.; Reif, M.; Kirsch, S. F. *Org. Lett.* **2005**, *7*, 3925. (h) Sherry, B. D.; Maus, L.; Laforteza, B. N.; Toste, D. *J. Am. Chem. Soc.* **2006**, *128*, 8132. (i) Zhang, L.; Sun, J.; Kozmin, S. A. *Adv. Synth. Catal.* **2006**, *348*, 2271. (j) Horino, Y.; Luzung, M. R.; Toste, F. D. *J. Am. Chem. Soc.* **2006**, *128*, 11364. (k) Gung, B. W.; Bailey, L. N.; Wonser, J. *Tetrahedron Lett.* **2010**, *51*, 2251.

(3) Sherry, B. D.; Toste, F. D. *J. Am. Chem. Soc.* **2004**, *126*, 15978.

(4) Krafft, M. E.; Hallal, K. M.; Vidhani, D. V.; Cran, J. W. *Org. Biomol. Chem.* **2011**, *9*, 7535.

(5) Unpublished results from the Krafft group.

(6) Nasveschuk, C. G.; Rovis, T. *Org. Biomol. Chem.* **2008**, *6*, 240.

(7) (a) Ferrier, R. J. *J. Chem. Soc., Perkin Trans. 1* **1979**, 1455. (b) Blattner, R.; Ferrier, R. J.; Haines, S. R. *J. Chem. Soc., Perkin Trans. 1* **1985**, 2413. (c) Barton, D. H. R.; Camara, J.; Dalko, P.; Gero, S. D.; Quiclet-Sire, B.; Stutz, P. *J. Org. Chem.* **1989**, *54*, 3764. (d) Barton, D. H. R.; Augy-Dorey, S.; Camara, J.; Dalko, P.; Delaumeny, J. M.; Gero, S. D.; Quiclet-Sire, B.; Stutz, P. *Tetrahedron* **1990**, *46*, 215.

(8) (a) Adam, S. *Tetrahedron Lett.* **1988**, *29*, 6589. (b) Laszlo, P.; Dudon, A. *J. Carbohydr. Chem.* **1992**, *11*, 587.

(9) (a) Nasveschuk, C. G.; Rovis, T. *Org. Lett.* **2005**, *7*, 2173. (b) Zhang, Y.; Reynolds, N. T.; Manju, K.; Rovis, T. *J. Am. Chem. Soc.* **2002**, *124*, 9720. (c) Zhang, Y.; Rovis, T. *Tetrahedron* **2003**, *59*, 8979−8987. (d) Frein, J. D.; Rovis, T. *Tetrahedron* **2006**, *62*, 4573. (e) Nasveschuk, C. G.; Jui, N. T.; Rovis, T. *Chem. Commun.* **2006**, 3119. (f) Nasveschuk, C. G.; Rovis, T. *Angew. Chem., Int. Ed.* **2005**, *44*, 3264.

(10) Nonoshita, K.; Banno, H.; Maruoka, K.; Yamamoto, H. *J. Am. Chem. Soc.* **1990**, *112*, 316.

(11) Nakamura, A.; Tokunaga, M. *Tetrahedron Lett.* **2008**, *49*, 3729.

(12) Bosch, M.; Handerson, S.; Schalf, M. *J. Carbohydr. Chem.* **2008**, *27*, 103.

(13) (a) Roithova, J.; Hrusak, J.; Schroder, D.; Schwarz, H. *Inorg. Chim. Acta* **2005**, *358*, 4287. (b) Roithovà, J.; Jankovà, Š.; Jašíkovà, L.; Vàňa, J.; Hybelbauerovà, S. *Angew. Chem.* **2012**, *124*, 8503. (c) Jašíkovà, L.; Roithovà, J. *Organometallics* **2012**, *31*, 1935.

(14) Zimmerman, H. E. *J. Am. Chem. Soc.* **1966**, *88*, 1564. Zimmerman, H. E. *J. Am. Chem. Soc.* **1966**, *88*, 1566. Zimmerman, H. E. *Acc. Chem. Res.* **1971**, *4*, 272. Zimmerman, H. E. *Tetrahedron* **1982**, *38*, 753. For a review see Dewar., M. J. S. *Angew. Chem., Int. Ed. Engl.* **1971**, *10*, 761 and references cited therein.

(15) Jiao, H.; Schleyer, P. v. R. *J. Phys. Org. Chem.* **1998**, *11*, 655. An educational recent discussion: Rzepa, H. S. *J. Chem. Educ.* **2007**, *84*, 1535.

(16) (a) Houk, K. N.; Gonzalez, J.; Li, Y. *Acc. Chem. Res.* **1995**, *28* (2), 81−90. (b) Houk, K. N.; Li, Y.; Evanseck, J. D. *Angew. Chem., Int. Ed. Engl.* **1992**, *31*, 682. (c) Dewar, M. J. S.; Jie, C. *Acc. Chem. Res.* **1992**, *25*, 537.

(17) Castro, A. M. M. *Chem. Rev.* **2004**, *104*, 2939.

(18) Becke, A. D. *J. Chem. Phys.* **1993**, *98*, 5648. Becke, A. D. *Phys. Rev. A* **1998**, *38*, 3098. Lee, C.; Yang, W.; Paar, R. G. *Phys. Rev. B* **1980**, *37*, 785.

(19) (a) Dunning, T. H.; Hay, P. J. In *Methods of Electronic Structure Theory*; Schaefer, H. F., III, Ed.; Plenum: New York, 1976; Vols. 2, 3, pp 1−28; (b) Hay, P. J.; Wadt, W. R. *J. Chem. Phys.* **1985**, *82*, 270. (c) Hay, P. J.; Wadt, W. R. *J. Chem. Phys.* **1985**, *82*, 284. (d) Hay, P. J.; Wadt, W. R. *J. Chem. Phys.* **1985**, *82*, 299. (e) Check, C. E.; Faust, T. O.; Bailey, J. M.; Wright, B. J.; Gilbert, T. M.; Sunderlin, L. S. *J. Phys. Chem. A* **2001**, *105*, 8111.

(20) Frisch, M. J.; Trucks, G. W.; Schlegel, H. B.; Scuseria, G. E.; Robb, M. A.; Cheeseman, J. R.; Montgomery, J. A., Jr.; Vreven, T.; Kudin, K. N.; Burant, J. C.; Millam, J. M.; Iyengar, S. S.; Tomasi, J.; Barone, V.; Mennucci, B.; Cossi, M.; Scalmani, G.; Rega, N.; Petersson, G. A.; Nakatsuji, H.; Hada, M.; Ehara, M.; Toyota, K.; Fukuda, R.; Hasegawa, J.; Ishida, M.; Nakajima, T.; Honda, Y.; Kitao, O.; Nakai, H.; Klene, M.; Li, X.; Knox, J. E.; Hratchian, H. P.; Cross, J. B.; Bakken, V.; Adamo, C.; Jaramillo, J.; Gomperts, R.; Stratmann, R. E.; Yazyev, O.; Austin, A. J.; Cammi, R.; Pomelli, C.; Ochterski, J. W.; Ayala, P. Y.; Morokuma, K.; Voth, G. A.; Salvador, P.; Dannenberg, J. J.; Zakrzewski, V. G.; Dapprich, S.; Daniels, A. D.; Strain, M. C.; Farkas, O.; Malick, D. K.; Rabuck, A. D.; Raghavachari, K.; Foresman, J. B.; Ortiz, J. V.; Cui, Q.; Baboul, A. G.; Clifford, S.; Cioslowski, J.; Stefanov, B. B.; Liu, G.; Liashenko, A.; Piskorz, P.; Komaromi, I.; Martin, R. L.; Fox, D. J.; Keith, T.; Al-Laham, M. A.; Peng, C. Y.; Nanayakkara, A.; Challacombe, M.; Gill, P. M. W.; Johnson, B.; Chen, W.; Wong, M. W.; Gonzalez, C.; Pople, J. A. *Gaussian 03*, Revision E.01; Gaussian: Wallingford, CT, 2004.

(21) Mauleon, P.; Krinsky, J. L.; Toste, F. D. *J. Am. Chem. Soc.* **2009**, *131*, 4513.

(22) (a) Lemiere, G.; Gandon, V.; Cariou, K.; Hours, A.; Fukuyama, T.; Dhimane, A.-L.; Fensterbank, L.; Malacria, M. *J. Am. Chem. Soc.* **2009**, *131*, 2993. (b) Tang, J.-M.; Bhunia, S.; Sohel, S.; Md., A.; Lin, M.-Y.; Liao, H.-Y.; Datta, S.; Das, A.; Liu, R.-S. *J. Am. Chem. Soc.* **2007**, *129*, 15677. (c) Xia, Y.; Dudnik, A. S.; Gevorgyan, V.; Li, Y. *J. Am. Chem. Soc.* **2008**, *130*, 6940. (d) Kovacs, G.; Ujaque, G.; Lledos, A. *J. Am. Chem. Soc.* **2008**, *130*, 853. (e) Alonso, I.; Trillo, B.; Lopez, F.; Montserrat, S.; Ujaque, G.; Castedo, L.; Lledos, A.; Mascarenas, J. L. *J. Am. Chem. Soc.* **2009**, *131*, 13020. (f) Cheong, P. H.-Y.; Morganelli, P.; Luzung, M. R.; Houk, K. N.; Toste, F. D *J. Am. Chem. Soc.* **2008**, *130*, 4517.

(23) (a) Jiao, H.; Schleyer, P.v. R. *Angew. Chem., Int. Ed. Engl.* **1993**, *32*, 1763. (b) Herges, R.; Jiao, H.; Schleyer, P. v. R. *Angew. Chem., Int. Ed. Engl.* **1994**, *33*, 1376. (c) Jiao, H.; Schleyer, P. v. R. *J. Chem. Soc., Perkin Trans.* **1994**, *2*, 407. (d) Jiao, H.; Schleyer, P. v. R. *J. Chem. Soc., Faraday Trans.* **1994**, *90*, 1559. (e) Jiao, H.; Schleyer, P. v. R. *J. Am. Chem. Soc.* **1995**, *117*, 11529. (f) Jiao, H.; Schleyer, P. v. R. *Angew. Chem., Int. Ed. Engl.* **1994**, *34*, 334.

(24) This assessment is to compare the aromatic character of pure organic analogous TS with the available prototypical TSs calculated at the B3LYP/6-311+G(d,p) level.

(25) (a) Yoo, H. Y.; Houk, K. N. *J. Am. Chem. Soc.* **1994**, *116*, 12047. (b) Wiest, O.; Black, K. A.; Houk, K. N. *J. Am. Chem. Soc.* **1994**, *116*, 10336 (see also ref 16).

(26) For a literature discussion of the connection between geometric asynchronicity and aromaticity, see: Fernandez, I.; Sierrra, M. A.; Cossio, F. P. *J. Org. Chem.* **2008**, *73*, 2083.

(27) In the prototypical Claisen rearrangement, chair (C_2h) TS is suggested to be more aromatic by the more negative NICS value (−25.4 ppm) relative to that for the boat (C_2v) TS (−22.7).[15]

(28) (a) Henry, P. M. *Acc. Chem. Res.* **1973**, 16. (b) Henry, P. M. *Adv. Organomet. Chem.* **1975**, *13*, 363.

(29) Overman, L. E. *Angew. Chem. Int. Ed. Engl.* **1984**, *23*, 579.

(30) (a) Baldwin, J. E.; Thomas, R. C.; Kruse, L. I.; Silberman, L. *J. Org. Chem.* **1977**, *42*, 3846. (b) Johnson, C. D. *Acc. Chem. Res.* **1993**, *26*, 476. For a recent critical analysis and refinement of the rules for alkyne cyclizations, see: Gilmore, K.; Alabugin, I. V. *Chem. Rev.* **2011**, *111*, 6513. Alabugin, I.; Gilmore, K.; Manoharan, M. *J. Am. Chem. Soc.* **2011**, *133*, 12608.

(31) (a) Takai, K.; Mori, I.; Oshima, K.; Nozaki, H. *Tetrahedron Lett.* **1981**, *22*, 3985. (b) Takai, K.; Mori, I.; Oshima, K.; Nozaki, H. *Bull. Chem. Soc. Jpn.* **1984**, *57*, 446. (c) Stevenson, J. W. S.; Bryson, T. A. *Tetrahedron Lett.* **1982**, *23*, 3143. (d) Takai, K.; Mori, I.; Oshima, K.; Nozaki, H. *Tetrahedron* **1984**, *40*, 4013. (e) Maruoka, K.; Saito, S.; Yamamoto, H. *J. Am. Chem. Soc.* **1995**, *117*, 1165.

(32) Interestingly, NBO analysis reveals that the interaction energies of $\pi(C_1-C_2) \rightarrow \sigma^*(C_3-O_4)$ ca. 33 and 8.6 kcal/mol, respectively, found for uncatalyzed and catalyzed TSs, indicate a greater hyperconjugative stabilization in the noncatalyzed TS. This is an illustration of greater acceptor ability of stretched bonds: (a) Gold, B.; Schevchenko, N.; Bonus, N.; Dudley, G. B.; Alabugin, I. V. *J. Org. Chem.* **2012**, *77*, 75. (b) Alabugin, I. V.; Gilmore, K.; Peterson, P. *Wiley Interdiscip. Rev.: Comput. Mol. Sci.* **2011**, *1*, 109.

(33) The presence of a donating *p*-NH₂-Ph substituent at C3 slightly facilitates C3−O4 bond elongation rendering the reaction less asynchronous. The electron acceptor, *p*-NO₂−Ph group has the opposite effect.

(34) For example: Electrophilic cyclizations. Stepanov, A. A.; Gornostaev, L. M.; Vasilevsky, S. F.; Arnold, E. V.; Mamatyuk, V. I.; Fadeev, D. S.; Gold, B.; Alabugin, I. V. *J. Org. Chem.* **2011**, *76*, 8737. Nucleophilic cyclizations. Baranov, D. S.; Vasilevsky, S. F.; Gold, B.; Alabugin, I. V. *RSC Adv.* **2011**, *1*, 1745. Vasilevsky, S. F.; Mikhailovskaya, T. F.; Mamatyuk, V. I.; Bogdanchikov, G. A.; Manoharan, M.; Alabugin, I. V. *J. Org. Chem.* **2009**, *74*, 8106. Vasilevsky, S. F.; Baranov, D. S.; Mamatyuk, V. I.; Gatilov, Y. V.; Alabugin, I. V. *J. Org. Chem.* **2009**, *74*, 6143. Radical cyclizations Alabugin, I. V.; Gilmore, K.; Patil, S.; Manoharan, M.; Kovalenko, S. V.; Clark, R. J.; Ghiviriga, I. *J. Am. Chem. Soc.* **2008**, *130*, 11535. Alabugin, I. V.; Manoharan, M. *J. Am. Chem. Soc.* **2005**, *127*, 9534. Alabugin, I. V.; Manoharan, M. *J. Am. Chem. Soc.* **2005**, *127*, 12583.

(35) Computations predicted that a Claisen rearrangement of unsymmetrical substrates proceeds via either an asynchronous concerted process or a step-by-step process: Borden, W. T.; Lonchairch, R. J.; Houk, K. N. *Ann. Rev. Phys. Chern.* **1988**, *39*, 213.

(36) (a) Burrows, C. J.; Carpenter, B. K. *J. Am. Chem. Soc.* **1981**, *103*, 6983. (b) Burrows, C. J.; Carpenter, B. K. *J. Am. Chem. Soc.* **1981**, *103*, 6984. (c) Gajewski, J. J.; Gee, K. R.; Jurayj, J. *J. Org. Chem.* **1990**, *55*, 1813.

(37) (a) Caramella, P.; Quadrelli, P.; Toma, L. *J. Am. Chem. Soc.* **2002**, *124*, 1130. (b) Quadrelli, P.; Romano, S.; Toma, L.; Caramella, P. *J. Org. Chem.* **2003**, *68*, 6035. (c) Caramella, P.; Quadrelli, P.; Toma, L.; Romano, S.; Khuong, K. S.; Northrop, B.; Houk, K. N. *J. Org. Chem.* **2005**, *70*, 2994.

(38) Roth, W. R.; Wollweber, D.; Offerhas, R.; Rekowski, V.; Lennartz, H. W.; Sustmann, R.; Müller, W. *Chem. Ber.* **1993**, *126*, 2701.

(39) (a) Hrovat, D. A.; Duncan, J. A.; Borden, W. T. *J. Am. Chem. Soc.* **1999**, *121*, 169. (b) Babinski, D. J.; Bao, X.; Arba, M. E.; Chen, B.; Hrovat, D. A.; Borden, W. T.; Frantz, D. E. *J. Am. Chem. Soc.* **2012**, *134*, 16139. (c) Bethke, S.; Hrovat, D. A.; Borden, W. T.; Gleiter, R. *J. Org. Chem.* **2004**, *69*, 3294. (d) Debbert, S. L.; Carpenter, B. K.; Hrovat, D. A.; Borden, W. T. *J. Am. Chem. Soc.* **2002**, *124*, 7896. (e) Duncan, J. A.; Azar, J. K.; Beathe, J. C.; Kennedy, S. R.; Wulf, C. M. *J. Am. Chem. Soc.* **1999**, *121*, 12029.

(40) Tantillo, D. J. *J. Phys. Org. Chem.* **2008**, *21*, 561. Nouri, D. H.; Tantillo, D. J. *J. Org. Chem.* **2006**, *71*, 3686.

(41) Such behavior of transition states is not unprecedented. Even more extreme examples are known. For example, a nonpericyclic 5-endodig cyclization was found to proceed via an aromatic transition state. Gilmore, K.; Manoharan, M.; Wu, J.; Schleyer, P.v.R; Alabugin, I. V. *J. Am. Chem. Soc.* **2012**, *134*, 10584.

(42) For a similar stabilization of zwitterionic intermediates in Pd- and Au-promoted [3,3] sigmatropic shifts, see: Siebert, M. R.; Tantillo, D. J. *J. Am. Chem. Soc.* **2007**, *129*, 8686. Felix, R. J.; Weber, D.; Gutierrez, O.; Tantillo, D. J.; Gagné, M. R. *Nat. Chem.* **2012**, *4*, 405. For other approaches to selective TS stabilization in alkyne reactions, see: (a) ref 32a. (b) Vasilevsky, S. F.; Mikhailovskaya, T. F.; Mamatyuk, V. I.; Bogdanchikov, G. A.; Manoharan, M.; Alabugin, I. V.

J. Org. Chem. **2009**, *74*, 8106. (c) Vasilevsky, S. F.; Gold, B.; Mikhailovskaya, T. F.; Alabugin, I. V. *J. Phys. Org. Chem.* **2012**, *25*, 998.

(43) B3LYP/LANL2DZ level gave higher value than B3LYP/6-311+G(d,p).

(44) (a) Borgulay, J.; Madeja, R.; Fahrni, P.; Hansen, H.-J.; Schmid, H.; Barner, R. *Helv. Chim. Acta* **1973**, *56*, 14. (b) Schmid, M.; Hansen, H.-J.; Schmid, H. *Helv. Chim. Acta* **1973**, *56*, 105. (c) Jolidon, S.; Hansen, H.-J. *Helv. Chim. Acta* **1977**, *60*, 978.

(45) Evans, D. A.; Golob, A. M. *J. Am. Chem. Soc.* **1975**, *97*, 4765. (b) Carpenter, B. K. *Tetrahedron.* **1978**, *34*, 1877. Evans, D. A.; Ballallargeon, D. J.; Nelson, J. V. *J. Am. Chem. Soc.* **1978**, *100*, 2242. For a recent study of analogous anionic oxy-Cope of bis-alkynes, see: (d) Pal, R.; Clark, R. J.; Manoharan, M.; Alabugin, I. V. *J. Org. Chem.* **2010**, *75*, 8689.

(46) For dissociative transition states in anionic [3,3] sigmatropic rearrangements, see: (a) Yoo, H.-Y.; Houk, K. N.; Lee, J. K.; Scialdone, M. A.; Meyers, A. I. *J. Am. Chem. Soc.* **1998**, *120*, 205. (b) Haeffner, F.; Houk, K. N.; Reddy, R.; Paquette, L. A. *J. Am. Chem. Soc.* **1999**, *121*, 11880. (c) Haeffner, F.; Houk, K. N.; Schulze, S. M.; Lee, J. K. *J. Org. Chem.* **2003**, *68*, 2310.

(47) See, also: (a) Black, K. A.; Wilsey, S.; Houk, K. N. *J. Am. Chem. Soc.* **1998**, *120*, 5622. (b) Hi, Y. Y.; Houk, K. N. *J. Am. Chem. Soc.* **1998**, *120*, 205. (c) Black, K. A.; Wilsey, S.; Houk, K. N. *J. Am. Chem. Soc.* **2003**, *125*, 6715.

(48) (a) Woodward, R. B.; Hoffmann, R. *J. Am. Chem. Soc.* **1965**, *87*, 2511. (b) Woodward, R. B.; Hoffmann, R. *Angew. Chem., Int. Ed. Engl.* **1969**, *8*, 781. (c) Berson, J. A.; Nelson, G. L. *J. Am. Chem. Soc.* **1967**, *89*, 5503. (d) Roth, W. R.; Friedrich, A. *Tetrahedron Lett.* **1969**, 2607. (e) Berson, J. A. *Acc. Chem. Res.* **1968**, *1*, 152.

(49) Our preliminary experimental studies of these external Lewis base effects were reported in ref 4.